Electrochemistry Communications 98 (2019) 73–77

Contents lists available at ScienceDirect

Electrochemistry Communications

journal homepage: www.elsevier.com/locate/elecom

Short communication

Atomic layer deposition of cobalt phosphate thin films for the oxygen evolution reaction

V. Di Palma[a,*], G. Zafeiropoulos[b], T. Goldsweer[a], W.M.M. Kessels[a], M.C.M. van de Sanden[a,b], M. Creatore[a], M.N. Tsampas[b]

[a] Department of Applied Physics, Eindhoven University of Technology, P.O. Box 513, 5600 MB Eindhoven, the Netherlands
[b] DIFFER, Dutch Institute for Fundamental Energy Research, P.O. Box 6336, 5600 HH Eindhoven, the Netherlands

ARTICLE INFO

Keywords:
Atomic layer deposition
Cobalt phosphate
Electrocatalysis
Oxygen evolution reaction

ABSTRACT

Electrodeposited cobalt phosphate has been reported as a valid alternative to noble metals as an electrocatalyst for the Oxygen Evolution Reaction (OER). In parallel, Atomic Layer Deposition (ALD) is increasingly being used in (photo)electrocatalytic applications. In this contribution we report on the electrocatalytic activity towards OER of ALD-prepared cobalt phosphate thin films. The selected ALD approach enables tuning of the Co-to-P atomic ratio, which is found to significantly affect the activity of the prepared electrocatalyst. Specifically, concurrently with a Co-to-P ratio increase from 1.6 to 1.9, the current density for OER increases from 1.77 mA/cm^2 at 1.8 V vs. RHE (Reversible Hydrogen Electrode) to 2.89 mA/cm^2 at 1.8 V vs. RHE. Moreover the sample with a Co-to-P ratio of 1.9 has superior performance when compared to electrodeposited cobalt phosphate thin films reported in the literature.

1. Introduction

Splitting water into hydrogen and oxygen is recognized as a viable approach to enable storage of renewable energy in the form of fuels. However, there are currently several issues hampering the development and implementation of this technology, one of which is the high cost associated with the use of noble-metal-based electrocatalysts [1–4]. In the last few decades much research has been dedicated to the synthesis of cost-effective electrocatalysts using cheaper transition metals [5]. In this regard, cobalt-based electrocatalysts currently show the most promising results [6]. In 2008 Kanan and Nocera [7] reported the preparation of a cobalt-phosphate-based electrocatalyst with good performance towards the oxygen evolution reaction (OER). Subsequently research on cobalt phosphate has been expanding by addressing the specific reaction mechanism for OER, the change in activity as a function of pH and for different buffer systems, and tuning properties in terms of coordination and crystal structure [6,8–13].

So far, the preparation of cobalt-phosphate-based electrocatalysts has been largely limited to (photo)electrodeposition in solution, implying that the control of the thickness is strongly related to the control of the current applied in the preparation of the electrocatalyst, and the composition is influenced by precursors, electrolytes and pH [14,15]. A higher level of control over material composition is expected to be achieved using atomic layer deposition (ALD), a thin film deposition technique based on the sequential dosing of gas phase reactants [16]. Because of its self-limiting growth behavior, ALD is characterized by thickness control at the atomic scale and excellent uniformity of the materials deposited [16–21]. Moreover, ALD generally allows the chemical composition of a material to be tuned by changing the ratio between the different dosing steps [22,23].

In the present work we use ALD to prepare cobalt phosphate thin films serving as electrocatalysts for OER. Three different types of samples have been prepared by ALD: one for cobalt oxide, one stoichiometric cobalt phosphate and one cobalt phosphate with a higher Co-to-P ratio. This approach makes it possible to explore the activity of the electrocatalyst as function of the stoichiometry.

2. Experimental

Cobalt phosphate and cobalt oxide thin films were deposited using a home-built ALD reactor described in detail elsewhere [24,25]. The reactor was equipped with a remote inductively coupled plasma generator (13.56 MHz). Bis(cyclopentadienyl)cobalt(II) ($CoCp_2$) and trimethyl phosphate (TMP, purity 97%), both purchased from Sigma-Aldrich, were used as precursors and O_2 plasma ($8.0{\cdot}10^{-3}$ mbar; 100 W) was used as reactant. A stainless steel bubbler containing $CoCp_2$ was

* Corresponding author.
E-mail address: v.d.palma@tue.nl (V. Di Palma).

https://doi.org/10.1016/j.elecom.2018.11.021
Received 31 October 2018; Received in revised form 29 November 2018; Accepted 29 November 2018
Available online 30 November 2018

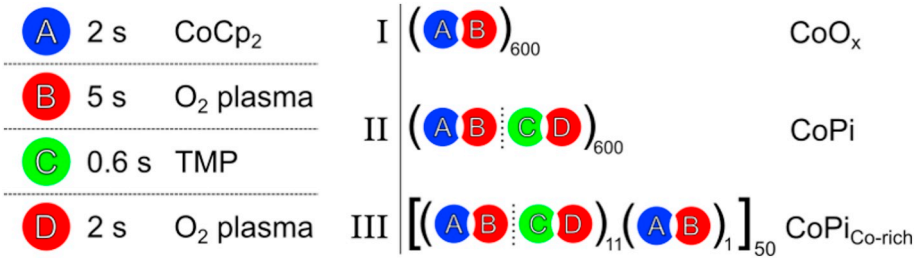

Fig. 1. Scheme of the dosing time used for each step (left) and ALD recipe used for CoO_x, CoPi and $CoPi_{Co\text{-}rich}$ (right). Each step of the process is self-limiting and the dosing times used are in saturation region.

Table 1
Elemental composition and density of the CoO_x, CoPi and $CoPi_{Co\text{-}rich}$ thin films from RBS measurements.

	Areal density (10^{15} atoms/cm^2)			Stoichiometry	Thickness from SE (nm)	Density of the thin film (g/cm^3)
	Co	P	O			
CoO_x	124 ± 4	–	176 ± 9	$Co_3O_{4.3}$	30 ± 2	5.6 ± 0.3
CoPi	127 ± 4	77 ± 3	(35 ± 2)·10	$Co_{3.2}P_2O_9$	67 ± 4	3.8 ± 0.2
$CoPi_{Co\text{-}rich}$	137 ± 4	71 ± 3	(33 ± 2)·10	$Co_{3.8}P_2O_{9.4}$	64 ± 4	4.1 ± 0.2

No carbon has been detected considering the sensitivity threshold of 4 atomic %.
Hydrogen detected from ERD is below 2 atomic % for both CoPi and $CoPi_{Co\text{-}rich}$ samples.

heated at 80 °C and the line from the bubbler to the reactor was kept at 100 °C. Ar (purity > 99.999%; base pressure $2.2{\cdot}10^{-2}$ mbar) was used as the carrier gas for $CoCp_2$ dosing. TMP was dosed in vapor-drawn mode by setting the temperature of the bubbler at 50 °C and the line from TMP bubbler to the reactor at 70 °C. The temperature of the wall of the reactor was set at 100 °C and the substrate holder at 300 °C. Three types of ALD recipes have been used for the preparation of the samples (Fig. 1): one for cobalt oxide (CoO_x), one for stoichiometric cobalt phosphate (CoPi) and one, given by the combination of the previous two, for cobalt phosphate with a higher Co-to-P ratio ($CoPi_{Co\text{-}rich}$). The dosing times and the ALD recipes used are reported in Fig. 1. A proper purge time has been used after each step (e.g. 7 s after oxygen plasma, 6 s after Co dosing and 2 s after TMP dosing). The detailed process characteristics (saturation curves, reaction mechanism, uniformity, etc.) will be reported in a separate publication.

Since cobalt is the reactive center providing electrocatalytic activity [8], the current measured in the OER depends on the number of cobalt atoms participating in the reactions. Moreover, the activity towards OER depends on the volume of cobalt phosphate, as reported in the literature [9]. For this reason, in order to study the activity as a function of the stoichiometric composition while minimizing the difference in activity due to the total amount of cobalt, we designed the ALD recipes using the same number of cobalt dosing steps (600 in total, see Fig. 1, right) for each sample, in order to keep the number of cobalt atoms approximately the same.

In situ spectroscopic ellipsometry (SE, Woollam M-2000) has been used to determine the thickness and refractive index of the layers when deposited on Si(100) single crystal. The Cauchy dispersion formula, which was found to be valid for cobalt phosphate, has been adopted to fit the experimental data. Rutherford backscattering spectrometry (RBS) has been performed for CoPi, $CoPi_{Co\text{-}rich}$ and CoO_x and elastic recoil detection (ERD) for the quantification of hydrogen for CoPi and $CoPi_{Co\text{-}rich}$. XPS was performed using the Thermo Scientific K-Alpha system, equipped with a monochromatic Al K_α x-ray source and the samples were analyzed as deposited.

The electrocatalytic activity of the layers towards OER were evaluated through cyclic voltammetry (CV), using a CompactStat-Ivium electrochemical workstation in a three-electrode configuration. Fluorine-doped tin oxide (FTO) on glass was used as a benchmark and as substrate for ALD of the electrocatalyst, which was used as a working anode with an area of 2 cm^2 immersed in the solution. A Pt mesh was the counter electrode and Ag/AgCl the reference electrode. A solution 0.1 M of KPi buffer (pH = 8) was used as the electrolyte for the CV measurements with a scan rate of 10 mV·s^{-1}. Impedance spectroscopy has been used to determine the cell resistance (~58 Ω) and 80% iR correction has been applied for the CV results. The potential measured is converted to reversible hydrogen electrode (RHE) using the formula: $V_{RHE} = V_{Ag/AgCl} + 0.1976\ V + 0.059 \times pH\ V$.

3. Results and discussion

Ellipsometric characterization of the processes used for the preparation of the three samples show a growth per cycle constant within the experimental error. The final thickness, reported in Table 1, is determined by fitting the ellipsometric data using a Cauchy dispersion formula for CoPi and $CoPi_{Co\text{-}rich}$ and an optical model employing a Gauss, a Tauc–Lorentz, and one Lorentz oscillator for CoO_x, as reported by Donders et al. [28], in the spectral range between 1.38 eV and 4.13 eV.

The three samples under study have been prepared by minimizing differences in the total areal density of Co (see Table 1) as determined by RBS. Table 1 also shows that the CoPi layer has a mass density comparable to bulk cobalt phosphate (3.8 g/cm^3 [26]) and a stoichiometry of $Co_{3.2}P_2O_9$ which is very close to the theoretical $Co_3P_2O_8$. The Co-to-P ratio of CoPi is found to be lower than that reported for electrocatalysts prepared by electrodeposition, generally exhibiting a Co-to-P ratio between 2 and 3 [7,9,15]. The sample $CoPi_{Co\text{-}rich}$ has a Co-to-P ratio higher than CoPi (1.9 vs. 1.6, respectively), as well as a higher mass density than CoPi (4.1 vs. 3.8 g/cm^3).

The oxidation state of Co and P for all layers is investigated by XPS (Fig. 2a–c). Co2p peaks show the characteristic features of Co^{+2} for both CoPi and $CoPi_{Co\text{-}rich}$, while CoO_x presents the features of the mixed oxide Co_3O_4 [27]. This agrees with what has been reported by Donders et al. [28] for CoO_x also prepared by ALD. The binding energy of the P2p peak (~133 eV) confirms that P is present in the oxidation state of a phosphate in both CoPi and $CoPi_{Co\text{-}rich}$ [29]. Moreover, the positions of the main peak and the satellite peak of the $Co2p_{3/2}$ signal are consistent with the peak positions reported in literature for cobalt phosphate [30,31], confirming the presence of cobalt phosphate in both CoPi and $CoPi_{Co\text{-}rich}$.

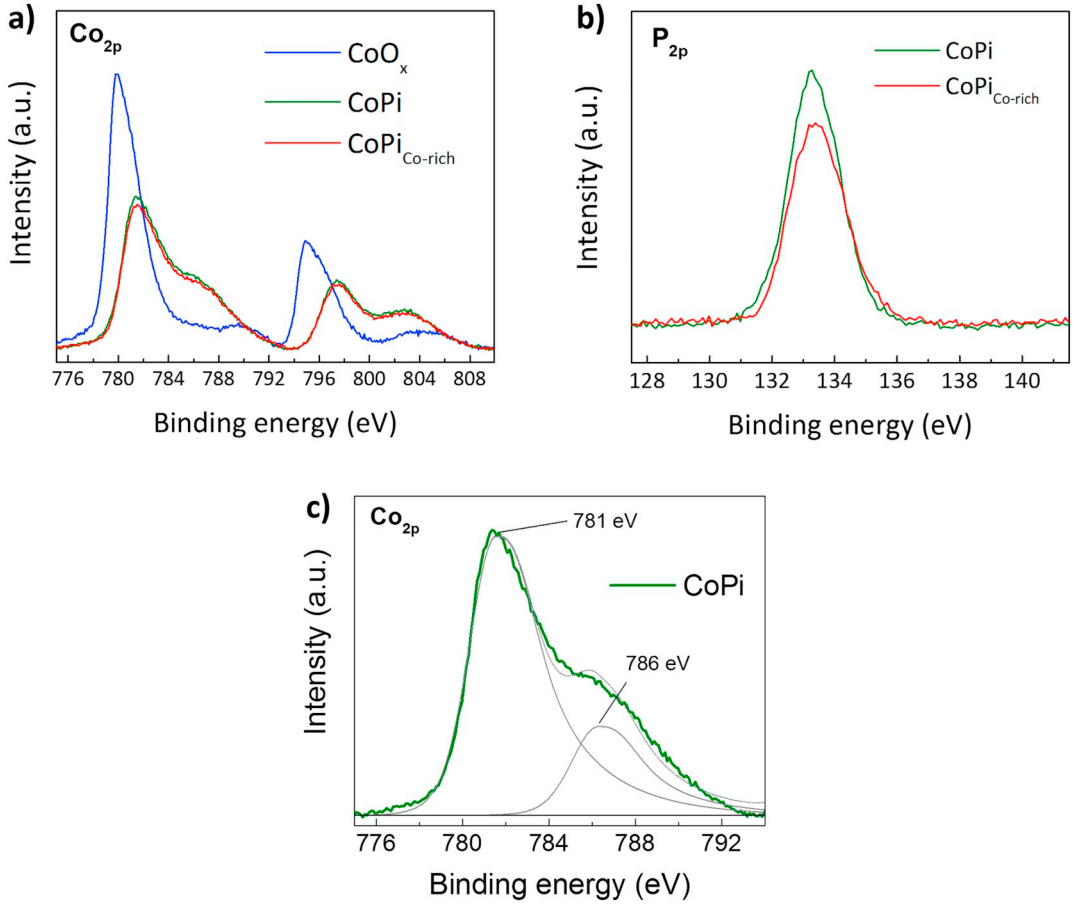

Fig. 2. XPS spectra of (a) Co2p for the three electrocatalysts and (b) P2p peaks for CoPi and $CoPi_{Co\text{-}rich}$. (c) Detail of the main peak (781 eV) and satellite peak (786 eV) of $Co2p_{3/2}$ signal for the CoPi sample.

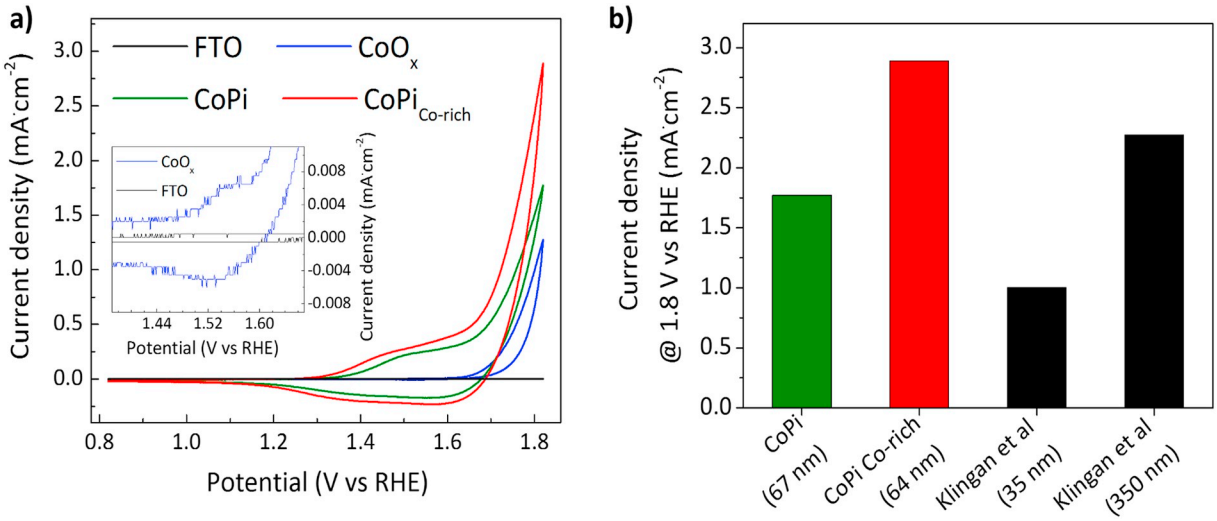

Fig. 3. (a) Cyclic voltammetry of the CoPi, $CoPi_{Co\text{-}rich}$ and CoO_x thin films, after 200 scans at 10 mV/s, in KPi buffer 0.1 M (pH = 8) after iR correction; (inset) detail of the oxidative/reductive wave for CoO_x. (b) Comparison of the current density values of CoPi and $CoPi_{Co\text{-}rich}$ (this work) at 1.8 V vs. RHE with those of reference [9].

X-ray diffraction analysis of the three layers did not provide any evidence of crystallinity in the samples. This is not unexpected, considering the literature on ALD of other metal phosphates, like iron phosphate [23], aluminum phosphate and titanium phosphate [32], which are not crystalline as deposited. Moreover, even electrodeposited cobalt-phosphate-based layers reported by Kanan and Nocera [7] and by Klingan et al. [9] turn out to be amorphous. The activity of the samples towards OER has been studied by CV (Fig. 3a). As expected, FTO has very poor activity towards OER, therefore it was selected as a substrate to test the ALD layers. By contrast, both CoPi and $CoPi_{Co\text{-}rich}$ show a high non-catalytic wave before the onset potential (< 1.6 V vs. RHE), which can be attributed to the oxidation of Co^{+2} [9,33]. The inset of Fig. 3a shows that CoO_x is also characterized by this feature, although at lower intensity than CoPi. The difference in intensity can be

explained in terms of the mixed oxidation state of cobalt in CoO_x, leading to approximately only 1/3 of the metallic centers undergoing oxidation. Furthermore, since the activity of cobalt phosphate also involves the bulk of the material, while this behavior is not reported in the literature for cobalt oxide, we can expect that only the surface of CoO_x will react and will be oxidized/reduced during the CV scan, while for CoPi the oxidation will involve a much larger number of cobalt centers [8,9]. This hypothesis is confirmed by the behavior of the $CoPi_{Co\text{-}rich}$ film, which presents a higher areal density of cobalt than CoPi (137 vs. $127 \cdot 10^{15}$ atoms/cm^2) and a higher current density (0.34 vs. 0.26 mA·cm^{-2} at 1.55 V vs. RHE) for Co^{+2} oxidation.

SEM top-view and cross-section analysis have been performed to exclude the influence of surface roughness on the activity. From SEM analysis, both CoPi and $CoPi_{Co\text{-}rich}$ samples are smooth and compact and no crystallites are visible. Therefore the activity towards OER of the three electrocatalysts can essentially be explained by considering the oxidation state of cobalt, the bulk reactivity and the different stoichiometry. The current density measured for CoPi at 1.8 V vs. RHE is 1.77 mA·cm^{-2}, while CoO_x reaches a current density 28% lower than CoPi at the same potential. Considering that both samples have a comparable areal density of cobalt, CoPi turns out to be more efficient because bulk cobalt centers are also electro-active. The sample $CoPi_{Co\text{-}rich}$ has the best performance with a current density of 2.89 mA·cm^{-2} at 1.8 V vs. RHE, which is 63% higher than CoPi. In view of the previous considerations, we attribute this improvement to the stoichiometry of this material. In the work of Surendranath et al. [8], higher current density at a lower potential is reached for a 40 nm thick electrocatalyst, in which the Co-to-P ratio is expected to be between 2 and 3, according to the deposition conditions they used [7,15]. Therefore the enhancement of the activity towards OER observed when the Co-to-P ratio increases from 1.6 (CoPi) to 1.9 ($CoPi_{Co\text{-}rich}$) is in line with the observation in literature, regardless of the difference in preparation method.

To better compare our results with those in the literature, it is important to consider the number of CV scans and range of scanning potential in view of their influence on the results. As reported by Gonzalez-Flores et al. [34], the current density generally increases with the number of CV scans for cobalt-phosphate-based electrocatalysts. Therefore, we have selected the work of Klingan et al. [9], which reports the same number of CV scans (200) and potential range used in our study. Fig. 3b shows a comparison, in terms of current density values for OER at 1.8 V vs. RHE, between ALD-prepared samples and the electrodeposited samples reported in [9]. The ALD $CoPi_{Co\text{-}rich}$ sample exhibits superior OER even when compared with thicker electro-deposited layers. Therefore, the ALD CoPi-based layers are interesting candidates for use in water splitting. The difference between the activities reported in [9] and this work may be due to the difference in material quality, specifically the presence of impurities. The electrodeposited cobalt-based electrocatalyst is reported to include impurities such as potassium, which has no role in the catalysis, in a 1:1 ratio with phosphorus [7,15], whereas ALD-prepared samples definitely show a negligible concentration of the most common impurities expected (mainly carbon and hydrogen in this case) from the ALD process.

4. Conclusion

In this contribution we study the electrocatalytic activity towards OER of ALD-prepared cobalt phosphate thin films. The ALD approach allows us to tune the Co-to-P atomic ratio, which strongly affects the activity of the prepared electrocatalysts. The current density value increases from 1.77 mA/cm^2 at 1.8 V vs. RHE to 2.89 mA/cm^2 at 1.8 V vs. RHE concurrently with a Co-to-P ratio increase from 1.6 to 1.9. The results highlight the role that stoichiometric composition of cobalt phosphate has on its activity, suggesting that tuning the Co-to-P ratio can be used as new approach to optimize the electrocatalyst for OER.

Acknowledgments

Authors acknowledge the TU/e-DIFFER impulse program and the CO_2-neutral-fuels (supported by NWO and Shell global solutions) programs for financial support.

References

[1] M. Gratzel, Photoelectrochemical cells, Nature 414 (2001) 334–338, https://doi.org/10.1038/35104607.
[2] N.S. Lewis, D.G. Nocera, Powering the planet: chemical challenges in solar energy utilization, Proc. Natl. Acad. Sci. U. S. A. 103 (2006) 15729–15735, https://doi.org/10.1073/pnas.0603395103.
[3] J. Barber, Photosynthetic energy conversion: natural and artificial, Chem. Soc. Rev. 38 (2009) 185–196, https://doi.org/10.1039/B802262N.
[4] D. Gust, T.A. Moore, A.L. Moore, Solar fuels via artificial photosynthesis, Acc. Chem. Res. 42 (2009) 1890–1898, https://doi.org/10.1021/ar900209b.
[5] J.D. Blakemore, R.H. Crabtree, G.W. Brudvig, Molecular catalysts for water oxidation, Chem. Rev. 115 (23) (2015) 12974–13005, https://doi.org/10.1021/acs.chemrev.5b00122.
[6] H. Kim, J. Park, I. Park, K. Jin, S.E. Jerng, S.H. Kim, K.T. Nam, K. Kang, Coordination tuning of cobalt phosphates towards efficient water oxidation catalyst, Nat. Commun. 6 (2015) 8253, , https://doi.org/10.1038/ncomms9253.
[7] M.W. Kanan, D.G. Nocera, In situ formation of an oxygen-evolving catalyst in neutral water containing phosphate and Co^{2+}, Science 321 (5892) (2008) 1072–1075, https://doi.org/10.1126/science.1162018.
[8] Y. Surendranath, M.W. Kanan, D.G. Nocera, Mechanistic studies of the oxygen evolution reaction by a cobalt-phosphate catalyst at neutral pH, J. Am. Chem. Soc. 132 (46) (2010) 16501–16509, https://doi.org/10.1021/ja106102b.
[9] K. Klingan, F. Ringleb, I. Zaharieva, J. Heidkamp, P. Chernev, D. Gonzalez-Flores, M. Risch, A. Fischer, H. Dau, Water oxidation by amorphous cobalt-based oxides: volume activity and proton transfer to electrolyte bases, ChemSusChem 7 (5) (2014) 1301–1310, https://doi.org/10.1002/c ssc.201301019.
[10] M. Barroso, A.J. Cowan, S.R. Pendlebury, M. Gratzel, D.R. Klug, J.R. Durrant, The role of cobalt phosphate in enhancing the photocatalytic activity of α-Fe_2O_3 toward water oxidation, J. Am. Chem. Soc. 133 (38) (2011) 14868–14871, https://doi.org/10.1021/ja205325v.
[11] R.S. Khnayzer, M.W. Mara, J. Huang, M.L. Shelby, L.X. Chen, F.N. Castellano, Structure and activity of photochemically deposited “CoPi” oxygen evolving catalyst on titania, ACS Catal. 2 (10) (2012) 2150–2160, https://doi.org/10.1021/cs3005192.
[12] Y. Wang, Y. Wang, R. Jiang, R. Xu, Cobalt phosphate − ZnO composite photocatalysts for oxygen evolution from photocatalytic water oxidation, Ind. Eng. Chem. Res. 51 (30) (2012) 9945–9951, https://doi.org/10.1021/ie2027469.
[13] Y. Pihosh, I. Turkevych, K. Mawatari, J. Uemura, Y. Kazoe, S. Kosar, K. Makita, T. Sugaya, T. Matsui, D. Fujita, M. Tosa, M. Kondo, T. Kitamori, Photocatalytic generation of hydrogen by core-shell WO_3/$BiVO_4$ nanorods with ultimate water splitting efficiency, Sci. Rep. 5 (2015) 11141, , https://doi.org/10.1038/srep11141.
[14] M.W. Kanan, Y. Surendranath, D.G. Nocera, Cobalt–phosphate oxygen-evolving compound, Chem. Soc. Rev. 38 (2009) 109–114, https://doi.org/10.1039/B802885K.
[15] Y. Surendranath, M. Dinca, D.G. Nocera, Electrolyte-dependent electrosynthesis and activity of cobalt-based water oxidation catalysts, J. Am. Chem. Soc. 131 (7) (2009) 2615–2620, https://doi.org/10.1021/ja807769r.
[16] S.M. George, Atomic layer deposition: an overview, Chem. Rev. 110 (1) (2009) 111–131, https://doi.org/10.1021/cr900056b.
[17] C. Marichy, M. Bechelany, N. Pinna, Atomic layer deposition of nanostructured materials for energy and environmental applications, Adv. Mater. 24 (8) (2012) 1017–1032, https://doi.org/10.1002/adma.201104129.
[18] S.C. Riha, B.M. Klahr, E.C. Tyo, S. Seifert, S. Vajda, M.J. Pellin, T.W. Hamann, A.B.F. Martinson, Atomic layer deposition of a submonolayer catalyst for the enhanced photoelectrochemical performance of water oxidation with hematite, ACS Nano 7 (3) (2013) 2396–2405, https://doi.org/10.1021/nn305639z.
[19] N.P. Dasgupta, C. Liu, S. Andrews, F.B. Prinz, P. Yang, Atomic layer deposition of platinum catalysts on nanowire surfaces for photoelectrochemical water reduction, J. Am. Chem. Soc. 135 (35) (2013) 12932–12935, https://doi.org/10.1021/ja405680p.
[20] Y. Lin, Y. Xu, M.T. Mayer, Z.I. Simpson, G. McMahon, S. Zhou, D. Wang, Growth of p-type hematite by atomic layer deposition and its utilization for improved solar water splitting, J. Am. Chem. Soc. 134 (12) (2012) 5508–5511, https://doi.org/10.1021/ja300319g.
[21] R. Liu, Y. Lin, L.Y. Chou, S.W. Sheehan, W. He, F. Zhang, H.J.M. Hou, D. Wang, Water splitting by tungsten oxide prepared by atomic layer deposition and decorated with an oxygen-evolving catalyst, Angew. Chem. Int. Ed. 50 (2) (2011) 499–502, https://doi.org/10.1002/anie.201004801.
[22] S. Keun Kim, G.-J. Choi, C.S. Hwang, Controlling the composition of doped materials by ALD: a case study for Al-doped TiO_2 films, Electrochem. Solid-State Lett. 11 (7) (2008) G27–G29, https://doi.org/10.1149/1.2909768.
[23] K.B. Gandrud, A. Pettersen, O. Nilsen, H. Fjellvåg, High-performing iron phosphate for enhanced lithium ion solid state batteries as grown by atomic layer deposition, J. Mater. Chem. A 1 (2013) 9054–9059, https://doi.org/10.1039/c3ta11550j.
[24] Y. Hajara, V. Di Palma, V. Kyriakouc, M.A. Verheijen, E.A. Baranova, P. Vernoux, W.M.M. Kessels, M. Creatore, M.C.M. van de Sanden, M.N. Tsampas, Atomic layer

deposition of highly dispersed Pt nanoparticles on a high surface area electrode backbone for electrochemical promotion of catalysis, Electrochem. Commun. 84 (2017) 40–44, https://doi.org/10.1016/j.elecom.2017.09.023.
[25] H.C.M. Knoops, A.J.M. Mackus, M.E. Donder, M.C.M. van de Sanden, P.H.L. Notten, W.M.M. Kessels, ALD of platinum and platinum oxide films, Electrochem. Solid-State Lett. 12 (2009) G34–G36, https://doi.org/10.1149/1.3125876.
[26] J.B. Anderson, E. Kostiner, M.C. Miller, J.R. Rea, The crystal structure of cobalt orthophosphate $Co_3(PO_4)_2$, J. Solid State Chem. 14 (4) (1975) 372–377, https://doi.org/10.1016/0022-4596(75)90058-4.
[27] M.C. Biesinger, B.P. Payne, A.P. Grosvenor, L.W.M. Lau, A.R. Gerson, R. St, C. Smart, Resolving surface chemical states in XPS analysis of first row transition metals, oxides and hydroxides: Cr, Mn, Fe, Co and Ni, Appl. Surf. Sci. 257 (2011) 2717–2730, https://doi.org/10.1016/j.apsusc.2010.10.051.
[28] M.E. Donders, H.C.M. Knoops, M.C.M. van de Sanden, W.M.M. Kessels, P.H.L. Notten, Remote plasma atomic layer deposition of Co_3O_4 thin films, J. Electrochem. Soc. 158 (4) (2011) G92–G96, https://doi.org/10.1149/1.3552616.
[29] B. Senthilkumar, Z. Khan, S. Park, I. Seo, H. Ko, Y. Kim, Exploration of cobalt phosphate as a potential catalyst for rechargeable aqueous sodium-air battery, J. Power Sources 311 (2016) 29–34, https://doi.org/10.1016/j.jpowsour.2016.02.022.
[30] Y.P. Zhu, T.Z. Ren, Z.Y. Yuan, Hollow cobalt phosphonate spherical hybrid as high-efficiency Fenton catalyst, Nanoscale 6 (2014) 11395–11402, https://doi.org/10.1039/c4nr02679a.
[31] G. Ai, R. Mo, H. Li, J. Zhong, Cobalt phosphate modified TiO_2 nanowire arrays as co-catalysts for solar water splitting, Nanoscale 7 (2015) 6722–6728, https://doi.org/10.1039/c5nr00863h.
[32] J. Hämäläinen, J. Holopainen, F. Munnik, M. Heikkilä, M. Ritala, M. Leskelä, Atomic layer deposition of aluminum and titanium phosphates, J. Phys. Chem. C 116 (9) (2012) 5920–5925, https://doi.org/10.1021/jp205222g.
[33] M. Risch, K. Klingan, F. Ringleb, P. Chernev, I. Zaharieva, A. Fischer, H. Dau, Water oxidation by electrodeposited cobalt oxides—role of anions and redox-inert cations in structure and function of the amorphous catalyst, ChemSusChem 5 (3) (2012) 542–549, https://doi.org/10.1002/c ssc.201100574.
[34] D. Gonzalez-Flores, I. Sanchez, I. Zaharieva, K. Klingan, J. Heidkamp, P. Chernev, P.W. Menezes, M. Driess, H. Dau, M.L. Montero, Heterogeneous water oxidation: surface activity versus amorphization activation in cobalt phosphate catalysts, Angew. Chem. Int. Ed. 54 (2015) 2472–2476, https://doi.org/10.1002/anie.201409333.